ELSEVIER

Polymer 42 (2001) 9393–9403

polymer

www.elsevier.com/locate/polymer

Copolymerization of ethylene and 1,5-hexadiene by stereospecific metallocenes in the presence of Al(iBu)$_3$/[Ph$_3$C][B(C$_6$F$_5$)$_4$]

Il Kim[a,*], Yong Shu Shin[a], Jin-Kook Lee[a], Nam Ju Cho[a], Jang-Oo Lee[a], Mi-Sook Won[b]

[a]*Department of Polymer Science and Engineering, Pusan National University, 30 Jangjeon-dong, Geumjeong-gu, Pusan 609-735, South Korea*
[b]*Korea Basic Science Institute, Pusan Branch, 30 Jangjeon-dong, Geumjeong-gu, Pusan 609-735, South Korea*

Received 14 November 2000; received in revised form 26 March 2001; accepted 2 May 2001

Abstract

Copolymerizations of ethylene (E) with 1,5-hexadiene (1,5-HD) has been carried out with *rac*-1,2-ethylenebis(1-indenyl)Zr(NMe$_2$)$_2$ [*rac*-(EBI)Zr(NMe$_2$)$_2$] and isopropylidene(cyclopentadienyl)(9-fluorenyl)ZrMe$_2$ (iPr(Cp)(Flu)ZrMe$_2$) compounds combined with Al(i-Bu)$_3$/[Ph$_3$C][B(C$_6$F$_5$)$_4$] as a cocatalyst system. Microstructures of copolymers were determined by ^{1}H, ^{13}C NMR, Raman spectroscopy and X-ray diffraction (XRD). The isospecific *rac*-(EBI)Zr(NMe$_2$)$_2$/Al(i-Bu)$_3$/[Ph$_3$C][B(C$_6$F$_6$)$_4$] catalyst showed much higher polymerization activity than syndiospecific iPr(Cp)(Flu)ZrMe$_2$/Al(i-Bu)$_3$/[Ph$_3$C][B(C$_6$F$_6$)$_4$] catalyst; however, the latter catalyst showed much higher comonomer reactivity, resulting in $r_E = 17.44$ and $r_{1,5\text{-HD}} = 0.02$($r_E \times r_{1,5\text{-HD}} = 0.35$), than the latter catalyst showing $r_E = 4.48$ and $r_{1,5\text{-HD}} = 0.12$($r_E \times r_{1,5\text{-HD}} = 0.54$). The 1,2-inserted 1,5-HD led to cyclic backbones by the intramolecular reaction. The intramolecular cyclization was independent of the polymerization temperature. Detailed investigation on the structure of copolymers by ^{13}C NMR and distortionless enhancement by polarization transfer (DEPT) spectroscopies showed that alternating structural units become predominant as the amount of 1,5-HD incorporated into the copolymer increased. The qualitative and quantitative analyses of the structure of copolymers were also made by XRD and Raman spectroscopy. © 2001 Published by Elsevier Science Ltd.

Keywords: Ethylene; 1,5-hexadiene; Copolymerization

1. Introduction

Polymerization of strained cyclic alkenes such as cyclobutene, cyclopentene, or norbornene by the metallocene compound combined with aluminoxane cocatalyst leads to crystalline poly(cycloolefin)s, which are not generally processed due to their high melting points and their insolubility in common organic solvents. By copolymerizations of these cyclic olefins with ethylene and α-olefins cycloolefin copolymers (COC) can be produced, representing a new class of thermoplastic amorphous materials [1–5]. Cycloolefin copolymers are characterized by stiffness, excellent transparency and very high, long-life service temperatures. They are solvent and chemical resistant and can be melt-processed. In combination with these properties, the copolymers are suitable materials for optical applications, such as compact discs, lenses, optical fibers, and films [4–6]. A drawback of ethylene/cyclic alkene copolymerization is low reactivity of cyclic alkenes with respect to that of ethylene.

Metallocene catalysts can be utilized to polymerize nonconjugated and conjugated dienes. A new class of cyclopolymerization with nonconjugated 1,5-dienes affording ring structures interfaced by methylene groups, was discovered by Waymouth et al. [7–13]. A 1,2-insertion of the terminal double bond into the metallocene carbon bond is followed by an intramolecular cyclization forming *cis*- and *trans*-cyclopentane with diisotactic or disyndiotactic conformation of either *cis*- or *trans*-rings.

In this sense, copolymerizations of olefin and nonconjugated dienes can be an alternative method to produce the attractive materials, COC. Marques et al. and Luft et al. studied the copolymerizations of ethylene (E) and 1,5-hexadiene (1,5-HD) with metallocene catalysts at high pressure of ethylene [14,15]. The copolymerization of ethylene and 1,5-HD and the terpolymerization of ethylene, styrene and 1,5-HD with constrained geometry catalyst were reported by Mülhaupt and coworkers [16]. Shiono et al. investigated the copolymerizations of propylene and 1,5-HD or 1,7-octadiene with various metallocene catalysts [17]. However, there are few results that report the effect of the stereospecificity of metallocene catalyst on the catalytic activity and 1,5-HD reactivity in the copolymerization of ethylene and 1,5-HD.

* Corresponding author. Tel.: +82-051-510-1432; fax: +82-051-513-7720.

0032-3861/01/$ - see front matter © 2001 Published by Elsevier Science Ltd.
PII: S0032-3861(01)00456-6

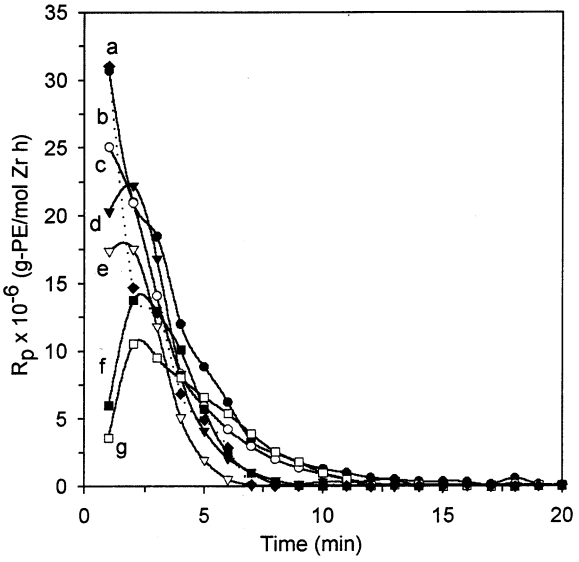

Fig. 1. R_p versus time curves obtained by the CAT-1/Al(i-Bu)$_3$/[Ph_3C][$B(C_6F_6)_4$] catalyst at various [1,5-HD]/[E] ratios of (a) 0, (b) 0.3, (c) 0.6, (d) 0.9, (e) 1.9, (f) 2.9, and (g) 3.7. Polymerization conditions: $P_{ethylene}$ = 5 psig, T_p = 30°C, [Al]/[Zr] = 80, [(Ph_3C)($B(C_6F_5)_4$)]/[Zr] = 1 and toluene = 80 ml.

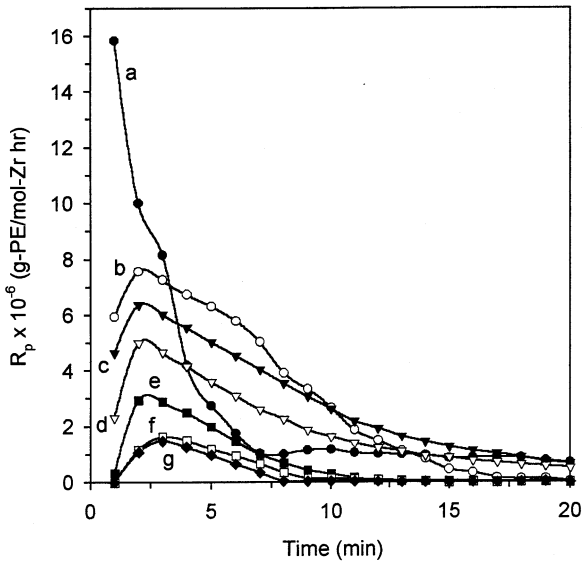

Fig. 2. R_p versus time curves obtained by the CAT-2/Al(i-Bu)$_3$/[Ph_3C][$B(C_6F_6)_4$] catalyst at various [1,5-HD]/[E] ratios of (a) 0, (b) 0.3, (c) 0.6, (d) 0.9, (e) 1.9, (f) 2.9, and (g) 3.7. Polymerization conditions: $P_{ethylene}$ = 5 psig, T_p = 30°C, [Al]/[Zr] = 80, [(Ph_3C)($B(C_6F_5)_4$)]/[Zr] = 1 and toluene = 80 ml.

In this study, we described the effect of metallocene stereospecificity on the kinetics of ethylene/1,5-HD copolymerizations with two metallocene catalysts, isospecific *rac*-1,2-ethylenebis(1-indenyl)Zr(NMe_2)$_2$ (*rac*-(EBI)Zr(NMe_2)$_2$, CAT-1) and syndiospecific isopropylidene(cyclopentadienyl)(9-fluorenyl)ZrMe_2 (*i*Pr(Cp)(Flu)ZrMe_2, CAT-2), combined with Al(i-Bu)$_3$/[Ph_3C][$B(C_6F_5)_4$] as a cocatalyst system. In addition, the microstructure of poly(ethylene-*co*-1,5-hexadiene) obtained by both catalysts was compared.

2. Experimental

2.1. Materials

All reactions were carried out under a purified nitrogen atmosphere using standard glove box and Schlenk techniques. Polymerization-grade ethylene (SK, Korea) was purified by passing it through columns of Fisher RIDOX catalyst and molecular sieve 5A/13X. 1,5-Hexadiene (Kumho Chemical, Korea) was distilled from CaH_2. Solvents were distilled from Na/benzophenone and stored over molecular sieves (4A). Triisobutyl aluminum (Al(i-Bu)$_3$) was obtained from Aldrich and used without further purification. Metallocene catalysts, *rac*-(EBI)Zr(NMe_2)$_2$ [18,19] and Me_2C(Cp)(Flu)ZrMe_2 [20], and anionic [Ph_3C][$B(C_6F_5)_4$] [21–23] compounds were synthesized according to literature procedures.

2.2. Copolymerization

Copolymerizations were carried out in a 250 ml glass reactor equipped with a magnetic stirrer and thermometer. In a dry box, the reactor was filled with 80 ml of toluene, Al(i-Bu)$_3$, 1,5-hexadiene, and metallocene compound and immersed in a constant-temperature bath previously set to a desired temperature. When the reactor temperature had been equilibrated to the bath temperature, ethylene was introduced into the reactor after pumping out nitrogen gas under vacuum. When no more absorption of ethylene into toluene was observed, a prescribed amount of [Ph_3C][$B(C_6F_5)_4$] dissolved in toluene was injected into the reactor and the polymerization was started. The polymerization rate was determined at every 0.01 s from the rate of consumption of ethylene, and was measured by a hot-wire flowmeter (model 5850 D, Brooks Instrument) connected to a personal computer through an analog to digital converter. Polymerization was quenched by the addition of methanol. The polymer obtained was filtered, washed with an excess amount of methanol and dried in vacuum at 50°C for 24 h. The vapour–liquid equilibrium for ethylene/1,5-HD/toluene mixture was calculated from the Soave–Redlich–Kwong equations [24–26]. This set of thermodynamic equations was selected among those available in HYSIS™ (commercialized by Hyprotech, Ver. 1.2) on the basis of a comparison with the experimental results. The concentration of the comonomer was, hence, calculated.

2.3. Characterization

^1H, ^{13}C NMR and distortionless enhancement by polarization transfer (DEPT) spectra of the copolymers were recorded at 120°C on a Varian Unity Plus 300 spectrometer. Samples were prepared by dissolving the copolymer in

$CDCl_3$-tetrachloroethane (1/5, v/v). By using the ACD/Labs Software from Advanced Chemistry Development, the peak assignment of the ^{13}C NMR spectra of the copolymers was made by comparing with the ^{13}C NMR spectra of cyclic homopolymer of 1,5-HD, poly(methylene-1,3,-cyclopentane) (PMCP) [27] and polyethylene.

Melting curves were recorded with a DuPont differential scanning calorimeter (DSC, Model 910) at 10°C/min. The intrinsic viscosities of polymers were determined in 1,2,4-trichlorobenzene at 135°C using an Ubbelohde viscometer. Raman spectra were recorded on a Brucker IFS55 FTIR spectrometer with the Raman modules (FRA 106), CaF_2 beam splitter, and Ge detector. The excitation source was a diode pumped Nd; YAG laser operated at 1064 nm. The laser power was 350 mW. X-ray diffraction (XRD) patterns of polymer powder were measured by a wide angle X-ray diffractometer (Rigaku 2013) using CuKα at 40 kV, 50 Ma with a scan speed of 2 2θ/min.

increasing [1,5-HD] as shown in Fig. 3. These results are different from those obtained from ethylene/α-olefin copolymerizations by using the same catalysts in that the addition of a specific amount of α-olefin generally accelerates the polymerization rate.

All polymerizations by CAT-1 and CAT-2 catalysts, especially in the presence of low HD, are marked by very high initial rates which reach $R_{p,max}$ within a few minutes after the start of polymerization. This demonstrates that the catalyst deactivation is completed within a few minutes after contacting zirconocenes with cocatalyst as shown below:

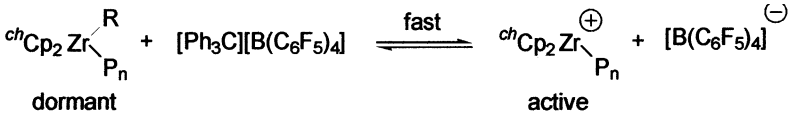

(1)

where $^{ch}Cp_2Zr$ is chiral *ansa*-zirconocene framework and P_n is a polymer chain. After the maximum rate is reached, fast decay starts. The mechanism involves reversible second-order deactivation combined with an irreversible deactivation of the active and/or dormant zirconium sites as follows:

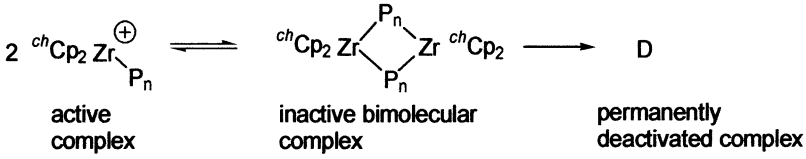

(2)

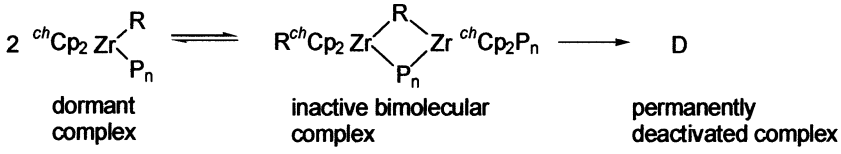

(3)

3. Results and discussion

3.1. Effect of 1,5-HD concentration

Copolymerizations of ethylene and 1,5-HD were carried out with CAT-1/Al(*i*-Bu)$_3$/[Ph_3C][$B(C_6F_6)_4$] and CAT-2/Al(*i*-Bu)$_3$/[Ph_3C][$B(C_6F_6)_4$] catalytic systems at 30°C by changing the 1,5-HD concentration. Figs. 1 and 2 show the rate profiles of copolymerization versus time obtained by CAT-1 and CAT-2, respectively. The polymerizations by CAT-1 (Fig. 1) reach a maximum rate ($R_{p,max}$) very rapidly and then decay very fast to almost zero rate within 10 min of polymerization. The polymerization rate (R_p) obtained by CAT-2 (Fig. 2) is relatively lower than those by CAT-1. The polymerizations by CAT-2 reach maximum rate within 3 min and then decay to a less degree than by CAT-1. The addition of comonomer makes the decay rate slow to some extent. Both catalytic systems show decrease of activity by

Mostly, the reversible second-order deactivation results from zirconocenes dimerization as illustrated in Eqs. (2) and (3) [28].

Other than kinetic factors diffusional limitations play some roles in the decay of polymerization rate. At the early period of polymerization, a pronounced change in the viscosity of the solvent was observed and the formation of fibrous polymer entangled on the stirrer was also noted. Evidently during this period, the growing active sites are encapsulated in precipitated polymer which may prevent monomers from diffusing into the active sites.

The amount of 1,5-HD incorporated into the copolymer was investigated by ^{13}C NMR analysis of the copolymers according to the literature procedures [14–16,27]. Fig. 4 shows the resulting copolymerization diagrams. A consistently higher incorporation of 1,5-HD was observed with syndiospecific CAT-2 than isospecific CAT-1. It is interesting to note that this tendency is in good agreement with the

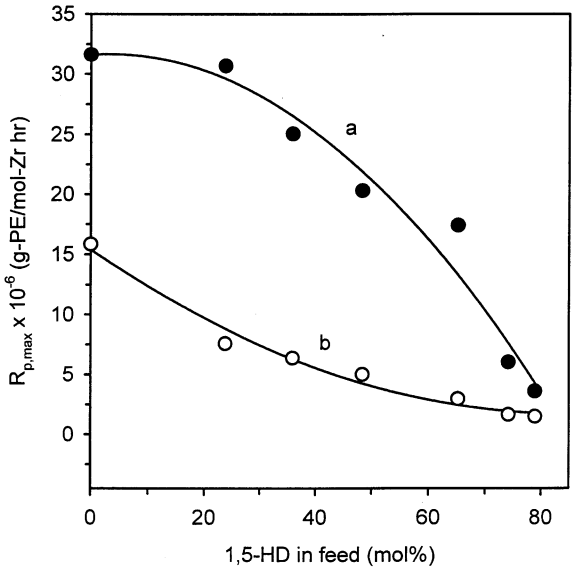

Fig. 3. Effect of 1,5-HD concentration on the maximum polymerization rate ($R_{p,max}$). Polymerization conditions are the same as those in Figs. 1 and 2, and the catalyst is (a) CAT-1 and (b) CAT-2.

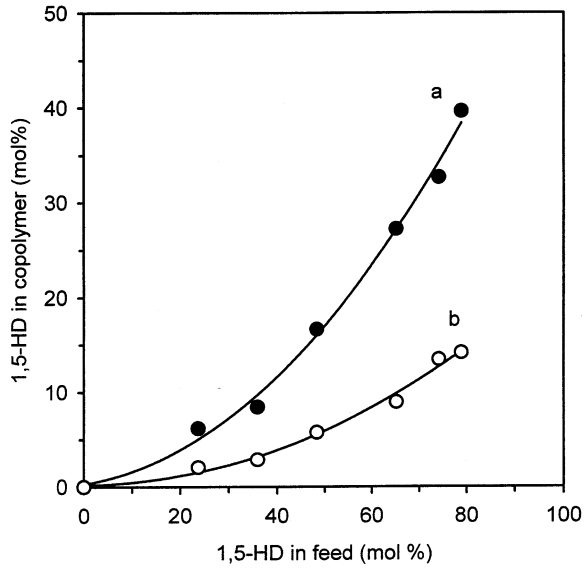

Fig. 4. Copolymerization diagrams of (a) CAT-2 and (b) CAT-1.

results of ethylene/α-olefin copolymerizations by the same catalysts, in which syndiospecific catalyst shows higher comonomer reactivity than isospecific catalyst. The calculation of copolymerization parameters according to Kelen-Tüdös plot by using the data in Fig. 4 and Table 1 resulted in $r_E = 17.44$ and $r_{1,5\text{-HD}} = 0.02 (r_E \times r_{1,5\text{-HD}} = 0.35)$ with CAT-1/Al(*i*-Bu)$_3$/[Ph_3C][$B(C_6F_6)_4$] catalyst, and $r_E = 4.48$ and $r_{1,5\text{-HD}} = 0.12 (r_E \times r_{1,5\text{-HD}} = 0.54)$ with CAT-2/Al(*i*-Bu)$_3$/[Ph_3C][$B(C_6F_6)_4$] catalyst.

An insight into the copolymer microstructure and the copolymerization mechanism can be realized from the reactivity ratios and their product. It is useful to recall that when $r_1 \times r_2 \approx 1$ the copolymer shows a random structure; when $r_1 \times r_2 > 1$ a blocky structure is evident and when $r_1 \times r_2 < 1$ the copolymer has an alternating structure. In this sense, poly(ethylene-*co*-1,5-HD) copolymers obtained in this study would appear to show a somewhat alternating structure, the more alternating the syndiospecific catalyst. However, detailed analysis of microstructure of the copolymers by ^{13}C NMR spectroscopy showed that CAT-1 produces copolymers of rather random distribution of 1,5-HD and CAT-2 produces copolymers of alternating distribution of 1,5-HD (vide infra). The 1,5-HD units incorporated in the copolymers produced by both catalysts was almost completely cyclized to yield cyclic units of methylene-1,3-cyclopentane (MCP) derived from the intramolecular cyclization of 1,2-added 1,5-HD.

The intrinsic viscosity of polymers determined in 1,2,4-trichlorobenzene at 135°C, decreased by the increase of 1,5-HD incorporated in copolymer (Table 1). The melting point (T_m) was evaluated from the DSC measurements. Ethylene homopolymers obtained by CAT-1 and CAT-2 catalysts show a T_m of 133.1 and 138.0°C, respectively, and 1,5-HD homopolymers obtained by CAT-1 and CAT-2 catalysts show a T_m of 85.0 and 76.7°C, respectively. The T_m-values of copolymers decreased monotonously by increasing the amount of 1,5-HD incorporated into the copolymer. All copolymers in this study showed melting peaks, demonstrating that they show semicrystalline structure. The double melting peaks appearing at higher concentration of 1,5-HD in copolymer also showed that the copolymers are polycrystalline. The structure of the copolymers is discussed below.

3.2. Effect of polymerization temperature (T_p)

The polymerization temperature is the most significant operational factor which affects the activity and the stereoselectivity of polymerization with metallocene catalysts. In this sense, copolymerizations of ethylene and 1,5-HD were carried out by using CAT-1/Al(*i*-Bu)$_3$/[Ph_3C][$B(C_6F_6)_4$] catalyst at various T_p by keeping the concentration of 1,5-HD in feed constant. Fig. 5 shows the rate profiles of copolymerization versus time and Table 1 summarizes the results of copolymerization. The polymerizations reach a maximum rate very rapidly and then decay very fast to almost zero rate within 10 min of polymerization without regard to T_p. The catalytic activity of homopolymerization of ethylene [29] or 1,5-HD [30] by using the same catalyst increased by increasing T_p within the range between 30 and 70°C. Thus, the decrease of the rate of copolymerization by increasing T_p, except a polymerization at 40°C, seems to be an unexpected result. The amount of 1,5-HD incorporated into the copolymer was increased from $[1,5\text{-HD}]_{\text{in copolymer}} = 8.59$ to 10.29 by increasing $T_p = 30$ to 40°C, and then decreased to 7.45 by further increasing T_p to 70°C. Detailed studies for the explanation of the reason

Table 1
Results of copolymerization of ethylene and 1,5-HD (polymerization conditions: $P_{ethylene}$ = 5 psig, [Al]/[Zr] = 80, [$(Ph_3C)(B(C_6F_5)_4)$]/[Zr] = 1 toluene = 80 ml)

Run no.	Cat.	[1,5-HD] in feed (mol%)	[Zr] (μmol)	T_p (°C)	[1,5-HD] in polymer[a] (mol%)	Cycl.[a] (%)	*trans*[b] (%)	$R_p \times 10^{-6}$[c]	T_m (°C)	δH_f (J/g)	$[\eta]$[d]	Composition of copolymer[e] (%)			X_c[f] (%)
												Block	Alt.	Random	
1	CAT-1	0	0.72	30	0	–	–	3.71	133.11	146.30	2.083	–	–	–	54.97
2		23.79	0.72	30	2.05	100	78.12	5.51	121.26	101.30	1.814	0	0	100	47.20
3		35.97	0.72	30	2.87	100	75.21	4.37	113.11	97.62	1.235	0	0	100	37.71
4		48.36	0.72	30	5.75	99.54	73.95	3.88	108.22	91.62	1.214	0	9.1	90.9	33.27
5		48.36	0.96	30	8.57	98.39	67.40	7.33	112.28	71.29	1.043	0	18.7	81.3	32.05
6		48.36	0.96	40	10.29	99.31	60.88	7.10	97.13, 116.16	85.43	0.889	0	18.0	82.0	34.35
7		48.36	0.96	50	8.59	99.45	65.86	5.27	96.10, 116.75	100.20	0.813	0	18.0	82.0	42.63
8		48.36	0.96	60	6.16	100	63.72	50.1	117.39	115.10	0.794	0	14.5	85.5	41.20
9		48.36	0.96	70	7.45	100	64.71	2.13	95.83, 116.91	105.40	0.716	0	9.9	90.1	40.22
10		65.19	0.72	30	8.93	98.54	64.17	2.77	99.99	73.36	0.880	0	16.7	83.3	32.09
11		74.17	0.72	30	13.43	97.99	66.67	2.64	87.04, 97.79	62.15	0.813	0	19.4	80.6	22.43
12		78.93	0.72	30	14.16	96.72	67.82	2.70	85.26, 96.77	52.73	0.696	0	22.5	77.5	21.43
13		100	3.12	25	100	97.99	62.89	–	84.97	11.52	0.365	–	–	–	–
14	CAT-2	0	1.53	30	0	–	–	2.80	137.95	131.30	2.203	–	–	–	49.55
15		23.79	1.53	30	6.18	99.53	65.10	3.06	105.63, 113.20	84.82	1.193	0	9.1	90.9	35.89
16		35.97	1.53	30	8.44	98.85	68.02	2.92	99.11, 118.99	65.12	1.177	0	11.5	88.5	29.61
17		48.36	1.53	30	16.67	97.51	67.42	2.00	88.57, 116.39	61.41	0.719	1.0	25.0	74.0	28.65
18		65.19	1.53	30	27.21	97.40	67.88	0.75	80.43, 115.11	35.69	0.523	7.4	35.4	57.2	26.55
19		74.17	1.53	30	32.67	97.24	67.42	0.41	76.73, 101.08	28.27	0.395	11.7	41.6	46.7	24.17
20		78.93	1.53	30	39.62	97.14	67.62	0.31	73.75, 96.91	22.01	0.368	19.1	46.8	34.1	23.02
21		100	3.12	25	100	97.69	67.64	–	76.69	12.39	0.352	–	–	–	–

[a] Cyclization determined by ^{1}H NMR.
[b] Determined by ^{13}C NMR.
[c] Average rate of polymerization by *g*-PE/mol-Zr hr.
[d] Measure in trichlorobenzene at 135°C.
[e] Calculated by the integration of ^{13}C NMR spectra of copolymers.
[f] Determined by XRD.

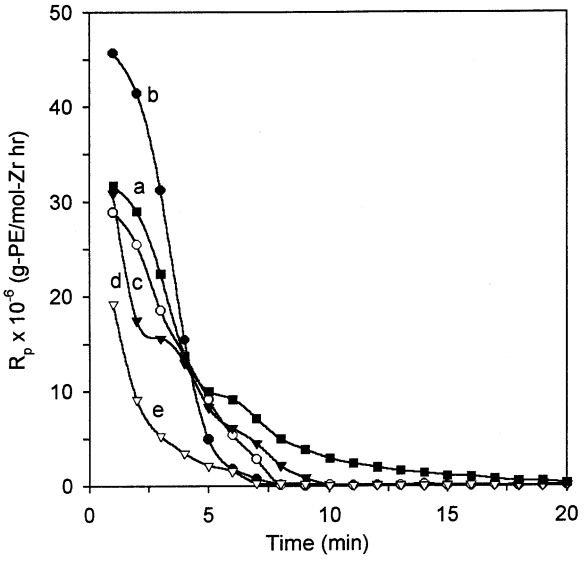

Fig. 5. R_p versus time curves obtained by the CAT-1/Al(i-Bu)$_3$/[Ph_3C][$B(C_6F_6)_4$] catalyst at various polymerization temperatures (T_p) of (a) 30, (b) 40, (c) 50, (d) 60, and (e) 70°C. Polymerization conditions: $P_{ethylene}$ = 5 psig, [Al]/[Zr] = 80, [(Ph_3C)($B(C_6F_5)_4$)]/[Zr] = 1, [1, 5-HD]/[E] = 0.9, and toluene = 80 ml.

why the comonomer reactivity changes according to T_p have to be carried out.

The strong dependence of the catalytic activity of zirconocene catalysts on the polymerization temperature was initially thought to be just the activation energy required for polymerization. When it was recognized that the active species is the zirconocenium ion, then one explanation for the polymerization temperature dependence could be that the activation energy needed to produce the ionic species because the zirconocene cation itself has a very low energy of activation for propagation, especially when the non-coordinating anion is utilized as a cocatalyst instead of MAO [22,23]. In this sense, the polymerization temperature range 30–70°C, employed in this study seems to be sufficiently high for the activation. As a result all polymerizations reach a maximum rate within a minute or so. However, all polymerizations decay rapidly to zero polymerization rate due to the irreversible deactivation of the active sites. In addition, precipitated polymer pronounced at the early period of polymerization limits the monomer diffusion into polymerization centers.

The melting behavior of the copolymer determined by DSC measurement was changed by the amount of 1,5-HD incorporated into the copolymer as shown in Section 3.1. The molecular weight of the copolymer decreased linearly by increasing T_p regardless of the variation of the amount of 1,5-HD incorporated into the copolymer. These results show that T_p is an important operational factor affecting the molecular weight even in copolymerization, since chain transfer reactions have higher activation energy than insertion, and thus a change in T_p strongly affects the molecular weight.

3.3. The microstructure of poly(ethylene-co-1,5-hexadiene)

The microstructure of ethylene/1,5-HD copolymers is considerably more complicated than that of simple ethylene/α-olefin copolymers since it includes cyclization of 1,2-added 1,5-HD. Cyclopolymerization of 1,5-HD giving PMCP is a chain growth reaction during which a conventional insertion of a vinylic function into the transition metal-carbon bond ([Zr-1,5-HD]*) is followed by an intramolecular insertion, resulting in the formation of

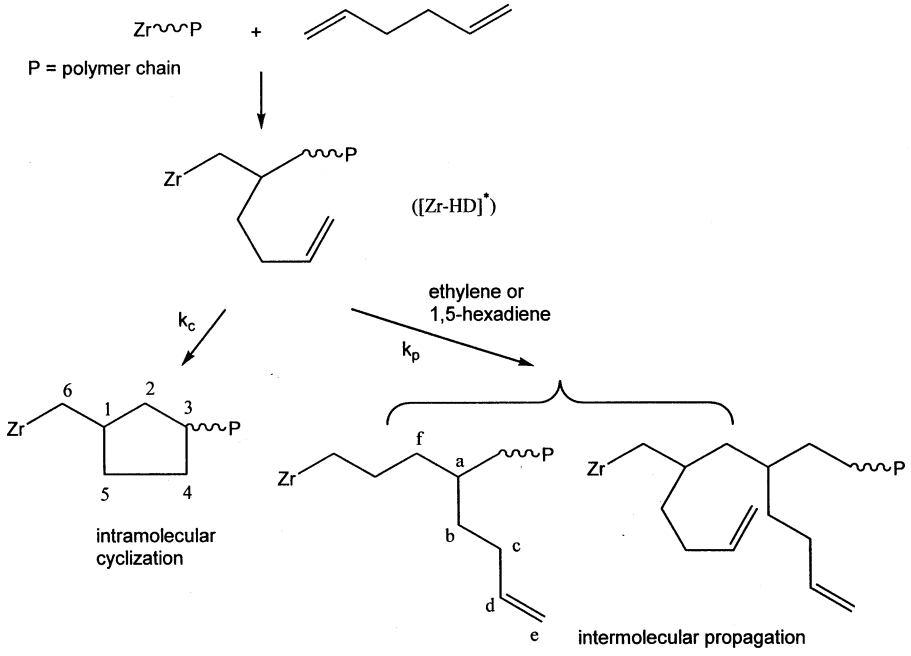

Scheme 1.

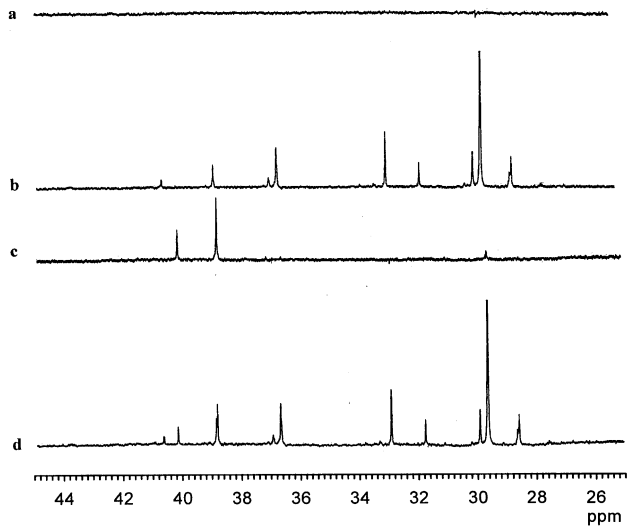

Fig. 6. DEPT spectra of (a) CH_3 carbons, (b) CH_2 carbons, (c) CH carbons, and ^{13}C NMR spectrum (d) of ethylene/1,5-HD copolymer produced by CAT-1 (Run No. 12 in Table 1).

alicyclic rings connected by methylene groups as shown in Scheme 1. The cyclic unit of 1,5-HD consisted of both the *cis*/*trans* stereochemistry of the rings and the relative stereochemistry between rings [7–13]. In addition, intermolecular propagation of 1,2-added 1,5-HD yields double bonds at the side chain of the copolymer. According to Scheme 1, the degree of cyclization of 1,2-inserted 1,5-HD is dependent upon the concentration of 1,5-HD in the feed due to the competition between intramolecular cyclization and intermolecular propagation reaction. However, the degree of cyclization of 1,2-inserted 1,5-HD determined by ^1H NMR spectroscopy of the copolymers obtained by CAT-1 and CAT-2 catalysts was not changed so much according to the variation of 1,5-HD concentration in the feed within our experimental range, i.e. only a small amount of vinylic double bonds in the side chain was detected by ^1H NMR spectra (4.85–5.02 ppm assigned to the resonance of $=CH_2$ and 5.5–5.9 ppm assigned to =CH) at a high concentration of 1,5-HD (Table 1).

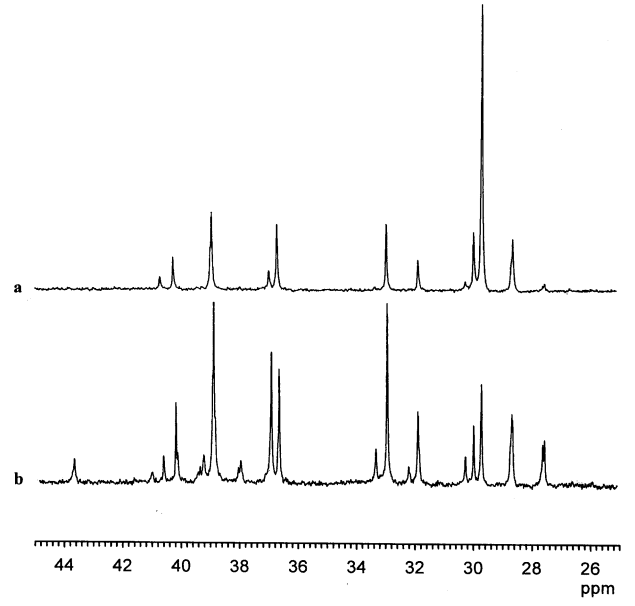

Fig. 7. ^{13}C NMR spectra of copolymers obtained with CAT-2: (a) Run No. 17 and (b) Run No. 20 in Table 1.

In order to get more insight into the microstructure of the copolymers obtained by CAT-1 and CAT-2 catalysts, the microstructure of copolymers was investigated with ^{13}C NMR spectroscopy together with DEPT spectroscopy. Fig. 6 shows the ^{13}C NMR and DEPT spectra of the copolymer produced by CAT-1 (Run No. 12 in Table 1) and Fig. 7 shows the ^{13}C NMR spectra of the copolymers synthesized by CAT-2 (Run No. 17 and 20 in Table 1). The stereochemistry in cyclopolymerization of 1,5-HD is dependent on the type of catalysts used. Waymouth and coworkers investigated the effect of metallocene geometry on the diastereoselectivity (selectivity of *cis*- or *trans*-cyclization) in the 1,5-HD homopolymerization and concluded that diastereoselectivity was affected by the steric effect of ligand and bite angle associated with the metallocene catalyst precursors [7]. Cavello et al. carried out conformational calculations on the diastereoselectivity and reported a good agreement with polymerization results [8]. DEPT spectroscopy (Fig. 7) confirms the existence of two methene resonance peaks originating from MCP units at 38.98 ppm, which is assigned to *trans* MCP units, and 40.32 ppm, which is assigned to *cis* structure of MCP units.[1] The resonance peaks at 31.84, 32.16, 32.92, 33.30, 38.04–38.06, 38.98, 39.00, 39.32, 39.45–39.49, 40.32, 40.74, and 41.12 ppm originated from various structures of MCP units[1]. The integration of the resonance of the peak at 32.92 ppm assigned to 4,5-*trans* (numbering in Scheme 1) and the peak at 31.84 ppm assigned to 4,5-*cis* reveals that both catalysts are characterized by a predominance of *trans* rings determined by diastereoselectivity of the intramolecular cyclization step (see also Table 1).

We may simplify the structure of the copolymers by considering the stereoregulations of isolated MCP units next to ethylene units as shown in Scheme 2. It can be observed that the reactivity of ethylene varies greatly

[1] The structure of poly(ethylene-*co*-1,5-hexadiene) has been interpreted by using ^{13}C NMR spectra as follows: The resonance peak at 43.85 ppm is assigned to homosequence units of MCP according to the ^{13}C NMR spectrum of homo-PMCP. The peaks at 32.16, 33.30, 38.04–38.06, 39.32, 39.45–39.49, and 41.12 ppm are assigned to *cis*-4,5, *trans*-4,5, *trans*-1,3, *trans*-2, *cis*-1,3, and *cis*-2 of homosequence units of MCP, respectively (numbering is in Scheme 1). The peaks at 31.84, 32.92, 38.98, 39.00, 40.32, and 40.74 ppm are assigned to *cis*-4,5, *trans*-4,5, *trans*-1,3, *trans*-2, *cis*-1,3, and *cis*-2 of isolated MCP units, respectively. The resonance peaks at 36.98, 36.71, 30.18, and 27.41 – 27.47 ppm in Fig. 8(b) are assigned to methylene carbons bonded to MCP rings of MCP-ethylene-MCP alternating units, to methylene carbons bonded to MCP rings of isolated MCP units, to center methylene carbons of MCP-ethylene-ethylene-MCP units, and to center methylene carbons of MCP-ethylene-MCP alternating units, respectively.

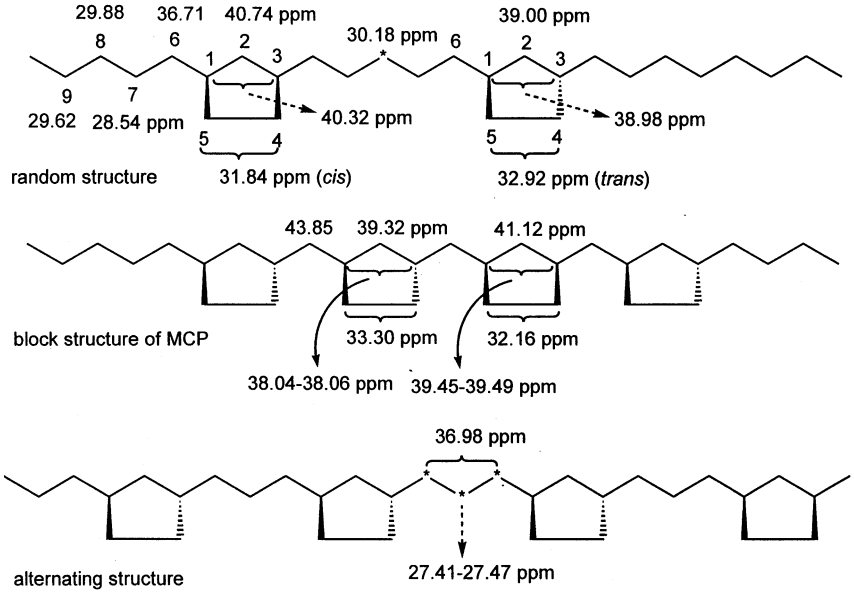

Scheme 2.

upon changing the catalyst stereospecificity and that the product of reactivity ratios ($r_E \times r_{1,5\text{-HD}}$) depends on such a catalyst feature: random, alternating or block copolymers can thus be synthesized by changing the catalyst ligands. Even if the value of the product of reactivity ratio shows kinetic structure of the copolymers, it cannot show detailed structure of the copolymer. If we assume that the appearance of the homosequential unit of MCP is a characteristic of block copolymer and the resonance peak of ethylene unit between two MCP units represents alternating structure (Scheme 2), we can estimate the detailed structure of the copolymers.

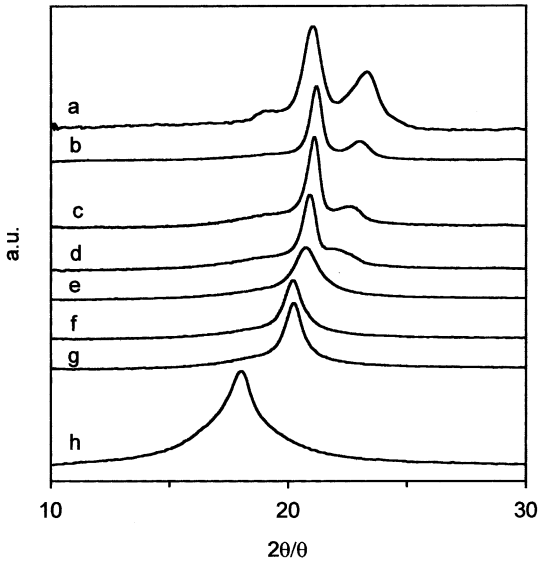

Fig. 8. XRD patterns of polyethylene (a), ethylene/1,5-HD copolymers [(b) Run No. 1 in Table 1, (c) Run No. 2, (d) Run No. 3, (e) Run No. 4, (f) Run No. 10, and (g) Run No. 11], and PMCP (h) produced by CAT-1/Al(*i*-Bu)$_3$/[Ph_3C][$B(C_6F_6)_4$] catalyst.

The copolymers synthesized by syndiospecific CAT-2 show complicated microstructures according to the comonomer concentration incorporated into the polymer as shown in Fig. 8. As the amount of 1,5-HD increases, the copolymers show diversified structure due to the complicated homosequence of MCP. Fig. 8(b) shows resonance peaks at 44.85 ppm, which does not appear in Fig. 8(a) and is assigned to the methylene peaks of homosequential units of MCP. The intensity of these peaks can be a measure of blocky character of copolymers. It is interesting to note that methylene peaks demonstrating the existence of alternating structure appear at 36.98 ppm. Isolated methylene peaks of MCP units, which can be a measure of random character of copolymers, appear at 36.71 ppm. If we integrate these three characteristic methylene resonance peaks, we can estimate the structural composition of copolymers.

As shown in Table 1, there are no homosequential units of MCP in copolymers obtained by using CAT-1. As the 1,5-HD amount incorporated into the copolymer increases, the composition of alternating structure increases. However, the overall structure of the copolymer obtained by CAT-1 seems to be random. On the other hand, the copolymers obtained by CAT-2 show diversified structure according to the amount of 1,5-HD. As the amount of 1,5-HD increases, the composition of both blocky and alternating structures increases. When $[1,5\text{-HD}]_{\text{in copolymer}} = 39.62$ the copolymer is composed of 19.1% of blocky structure, 46.8% of alternating structure, and 34.1% of random structure. Deciding only by $r_E \times r_{1,5\text{-HD}}$ value, CAT-1 ($r_E \times r_{1,5\text{-HD}} = 0.35$) produces a copolymer of more alternating character than CAT-2 ($r_E \times r_{1,5\text{-HD}} = 0.54$). However, the results obtained by the detailed investigation of the structure of the copolymers shows that the simple conclusion made on

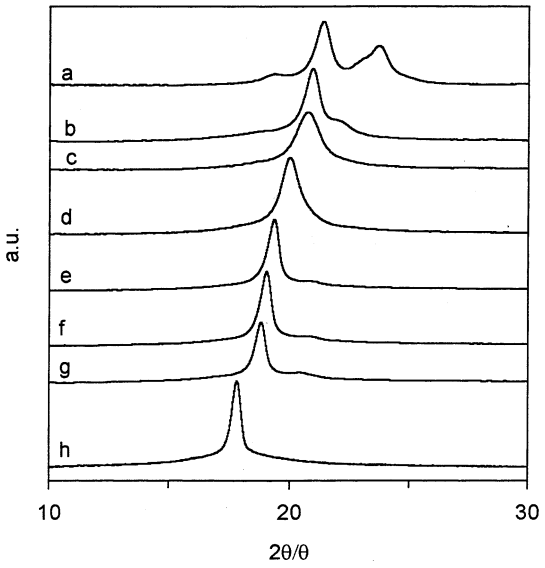

Fig. 9. XRD patterns of polyethylene (a), ethylene/1,5-HD copolymers [(b) Run No. 15 in Table 1, (c) Run No. 16, (d) Run No. 17, (e) Run No. 18, (f) Run No. 19, and (g) Run No. 20], and PMCP (h) produced by CAT-2/Al(i-Bu)$_3$/[Ph_3C][$B(C_6F_6)_4$] catalyst.

the structure of the copolymers by the product of reactivity ratios is somewhat obscure.

The vinylic double bonds in the side chain of the copolymers caused by the intermolecular propagation of 1,5-HD were not detected by ^{13}C NMR spectra. Considering the fact that they were detected by ^{1}H NMR spectra, the double bonds disappeared predominantly by crosslinking during ^{13}C NMR measurement at high temperature.

3.4. X-ray diffraction and Raman spectroscopy

As already discussed, the copolymers containing a large amount of 1,5-HD showed multiple melting peaks, demonstrating a polymorphism. In order to investigate the polymorphism phenomenon and crystallinity, we measured the XRD spectra of the copolymers. Figs. 8 and 9 show the spectra of copolymers obtained by CAT-1 and CAT-2, respectively. The spectra of homopolymers, polyethylene and PMCP, are also shown for comparison. As shown in Fig. 8, as the amount of 1,5-HD increases, the intensity of the peaks, which is a measure of crystallinity, becomes weak, and in the end all peaks except the peak at $2\theta = 21.03°$, disappeared. The crystallinity of copolymers calculated by the integration of the peaks is summarized in Table 1. It is interesting to note that the peak of polyethylene at 21.03° shifts downward as the amount of 1,5-HD increases (see Table 2). This phenomenon is shown clearly in Fig. 9 obtained by CAT-2. Downward shifting of the peaks means an increase of d-value and the change of crystal structure due to the introduction of MCP units into polymer backbone. Considering that there were two melting peaks which decrease as the amount of 1,5-HD increases (Table 1) and the ratio of alternating structure increased as the amount of 1,5-HD increases, it may be assumed that cocrystallization of MCP units with ethylene units causes a change of crystalline structure of polyethylene as well as a decrease of crystallinity. As shown in Fig. 9(e)–(g), the copolymers containing a large amount of 1,5-HD produced by CAT-2 show new XRD peaks at the 2θ value of 20.95 (e), 20.84 (f), and 20.46 (g). The integration of the individual peak yields 2:3:4 ratio. According to the estimation based on ^{13}C NMR spectra of these three copolymers, the ratio of alternating structure was 25.0:35.4:41.6 (Table 1). Thus, it may be said that the new peaks are characteristic ones induced by the alternating structure.

Table 2
Analysis of XRD shift of poly(ethylene-*co*-1,5-HD)

Run no.	[1,5-HD] in copolymer (%)	2θ	d-value
1	0	21.03	4.22
2	2.05	21.20	4.19
3	2.87	21.11	4.21
4	5.75	20.92	4.24
10	8.93	20.74	4.28
11	13.43	20.20	4.39
12	14.16	20.23	4.39
13	100	18.04	4.91
14	0	21.37	4.15
15	6.18	20.93	4.24
16	8.44	20.74	4.28
17	16.67	19.99	4.44
18	27.21	19.36	4.58
19	32.67	19.05	4.65
20	39.62	18.83	4.71
21	100	17.82	4.97

Raman spectroscopy has been used extensively for the analysis of polyethylene samples. Use has been made of the low-wavenumber longitudinal acoustic vibrations to determine lamellae thickness [31] and attempts have been made to quantify polymer crystallinity using features in the fingerprint region of the spectrum between 1000 and 1600 cm^{-1} [32]. In order to check the usefulness of Raman spectroscopy for the qualitative and quantitative structural analyses of copolymers, we recorded the Raman spectra of polyethylene, PMCP, and copolymers. Figs. 10 and 11 show the Raman spectra of the polymers produced by using **1** and **2**, respectively. Figs. 10(a) and 11(a) show typical Raman spectra of high-density polyethylene in the 700–1700 cm^{-1} spectral region. The Raman spectrum of polyethylene in the range 1000–1600 cm^{-1} can be subdivided into three main regions: (1) C–C stretching vibrations in the 1000–1150 cm^{-1} region, (2) –CH_2– twisting vibrations at ca. 1300 cm^{-1}, and (3) –CH_2– deformation, among which, wagging vibrations are between 1350 and 1500 cm^{-1} [33,34].

The amorphous part of the copolymer increases as the content of MCP units incorporated into the copolymer increases. This fact can be identified by the decrease of crystalline peak of polyethylene (1170 and 1417 cm^{-1}) and the increase of amorphous peak of polyethylene

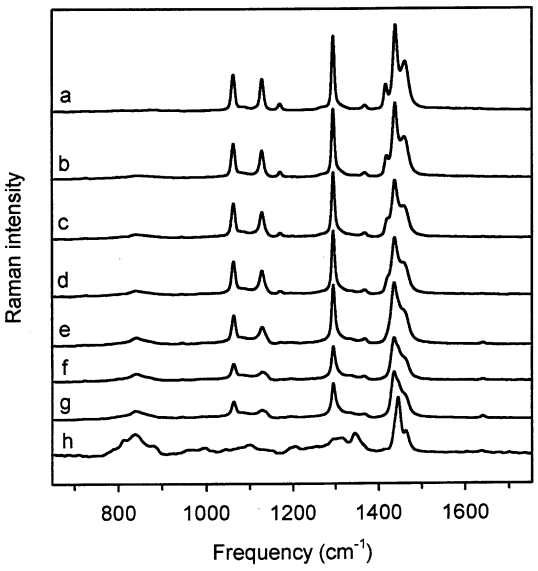

Fig. 10. Raman spectra of polyethylene (a), ethylene/1,5-HD copolymers [(b) Run No. 1 in Table 1, (c) Run No. 2, (d) Run No. 3, (e) Run No. 4, (f) Run No. 10, and (g) Run No. 11], and PMCP (h) produced by CAT-1/Al(*i*-Bu)$_3$/[Ph$_3$C][B(C$_6$F$_6$)$_4$] catalyst.

(1080 cm^{-1}). The peaks at 1640 are from C=C stretching vibration, which comes from vinylic double bonds of 1,2-inserted 1,5-HD. As the concentration of 1,5-HD in the feed increases, the cyclization of 1,2-inserted 1,5-HD was incomplete (Table 1). Thus, the peak appeared only at copolymers produced in the presence of high concentration of 1,5-HD (Figs. 10(e)–(g) and 11(e)–(g)). The peaks between 712 and 906 cm^{-1}, which are not discovered in polyethylene spectra, come from C–C vibration of the MCP unit. The intensities in these regions increase as the amount of 1,5-HD incorporated into the copolymer increase. Thus, the peaks between 712 and 906 cm^{-1} can be utilized for the quantitative analysis to measure the composition of copolymer. Fig. 12 shows the plots of intensity ratio versus the amount of 1,5-HD in copolymer measured by ^{13}C NMR spectroscopy. The intensity ratios were calculated by dividing the integral value of the peaks in the range between 712 and 906 cm^{-1} by the integral value of various reference peaks (block region of 1036–1165, 1261–1388, and 1388–1534 cm^{-1}). All copolymers are on the same straight line, demonstrating that Raman spectroscopy may not be a useful tool to differentiate a delicate microstructure of copolymers. However, it can be successfully used to estimate the rough composition of the copolymers as shown in Fig. 12.

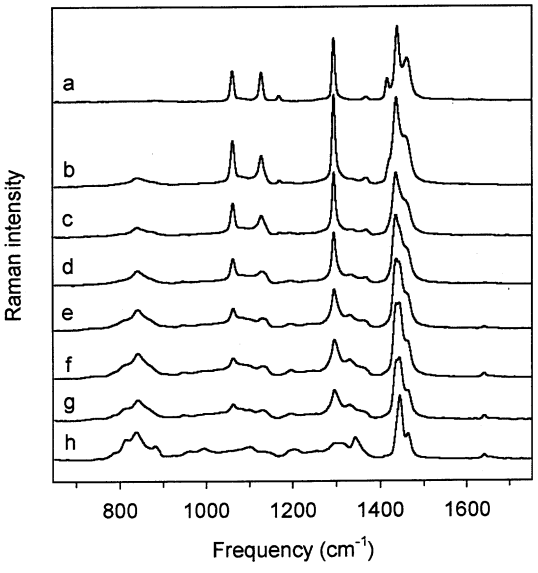

Fig. 11. Raman spectra of polyethylene (a), ethylene/1,5-HD copolymers [(b) Run No. 15 in Table 1, (c) Run No. 16, (d) Run No. 17, (e) Run No. 18, (f) Run No. 19, and (g) Run No. 20], and PMCP (h) produced by CAT-2/Al(*i*-Bu)$_3$/[Ph$_3$C][B(C$_6$F$_6$)$_4$] catalyst.

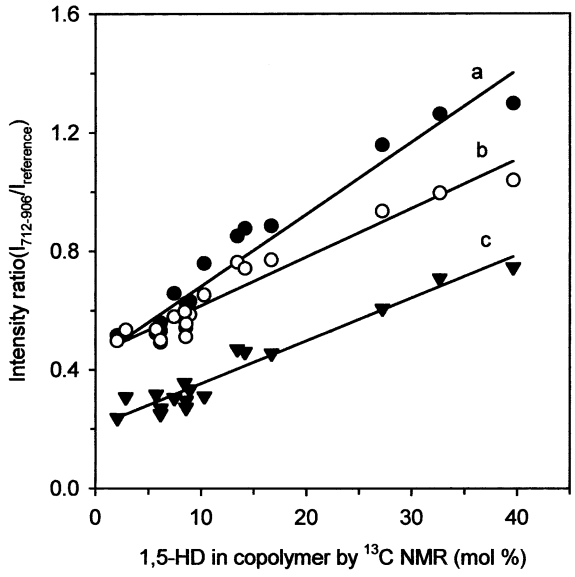

Fig. 12. Plots of intensity ratios of Raman spectroscopy versus 1,5-HD content in copolymer estimated by ^{13}C NMR: ratio of the integrating value of the peaks between 712 and 906 cm^{-1} to the integrating value of various reference peaks, block region of (a) 1036–1165 cm^{-1}, (b) 1261–1388 cm^{-1}, and (c) 1388–1534 cm^{-1}.

4. Conclusion

The isospecific CAT-1/Al(*i*-Bu)$_3$/[Ph$_3$C][B(C$_6$F$_6$)$_4$] catalyst showed a much higher polymerization activity than CAT-2/Al(*i*-Bu)$_3$/[Ph$_3$C][B(C$_6$F$_6$)$_4$] catalyst; however, CAT-2 showed much higher comonomer reactivity ($r_E = 17.44$, $r_{1,5\text{-HD}} = 0.02$, and $r_E \times r_{1,5\text{-HD}} = 0.35$) than CAT-1 ($r_E = 4.48$, $r_{1,5\text{-HD}} = 0.12$, and $r_E \times r_{1,5\text{-HD}} = 0.54$). The diastereoselectivity of the intramolecular cyclization reaction of 1,2-inserted 1,5-HD was independent of the stereospecificity of metallocene compounds, such that the cyclization of the 1,2-inserted 1,5-HD was almost complete in the copolymerizations by both CAT-1 and CAT-2 catalysts. The intramolecular cyclization was also independent of the polymerization temperature. Detailed investigation on the structure of copolymers by ^{13}C NMR spectroscopy

showed that the ratio of alternating structural unit become predominant as the amount of 1,5-HD incorporated into the copolymer increased for both catalytic systems. The qualitative and quantitative analyses of the structure of copolymers were also made by XRD and Raman spectroscopy, demonstrating that the copolymers containing a large amount of 1,5-HD showed polymorphism due to the development of alternating structure. Raman spectroscopy was a useful tool to estimate the rough composition of copolymers.

Acknowledgements

This work was supported by Korea Research Foundation Grant (KRF-2000-E00363).

References

[1] Kaminsky W, Bark A, Steiger R. J Mol Catal 1992;74:109.
[2] Kaminsky W, Noll A. Polym Bull (Berlin) 1993;31:175.
[3] Kaminsky W, Bark A, Arndt M. Makromol Chem Macromol Symp 1991;47:83.
[4] Cherdron H, Brekner MJ, Osan F. Angew Makromol Chem 1994;223:121.
[5] Kaminsky W. Macromol Chem Phys 1996;197:3907.
[6] Land HT. Proceedings of International Congress on Metallocene Polymers. Brussels: Scotland Business Research Incorporation, 1995 p. 217.
[7] Coates GW, Waymouth RM. J Am Chem Soc 1993;115:91.
[8] Cavallo L, Guerra G, Corradini P, Resconi L, Waymouth RM. Macromolecules 1993;26:260.
[9] Kesti MR, Waymouth RM. J Am Chem Soc 1992;114:3565.
[10] Coates GW, Waymouth RM. J Mol Catal 1992;76:189.
[11] Mogstad A, Waymouth RM. Macromolecules 1992;25:2282.
[12] Coates GW, Waymouth RM. J Am Chem Soc 1991;113:6270.
[13] Resconi L, Waymouth RM. J Am Chem Soc 1990;112:4953.
[14] Coutinho FMB, Marques MFV. Polim Cienc Technol 1993;3:20.
[15] Bergemann C, Cropp R, Luft G. J Mol Catal A Chem 1997;116:323.
[16] Sernetz FG, Mülhaupt R, Waymouth RM. Polym Bull 1997;38:141.
[17] Naga N, Shiono T, Ikeda T. Macromolecules 1999;32:1348.
[18] Jordan RF, Diamond GM. WO 9532979, 1995.
[19] Diamond GM, Rodewald S, Jordan RF. Organometallics 1995;15:4038.
[20] Ewen JA, Jones RL, Razavi A, Ferraa JD. J Am Chem Soc 1988;110:6255.
[21] Ewen JA, Elder M. J Makromol Chem Macromol Symp 1993;66:179.
[22] Chien JCW, Tsai WM. Makromol Chem Macromol Symp 1993;66:141.
[23] Chien JCW, Xu B. Makromol Chem Rapid Commun 1993;14:109.
[24] Soave G. Chem Engng Sci 1972;27:1196.
[25] Peneloux A, Rauzy E, Freze R. Fluid Phase Eq 1982;8:7.
[26] Schwartzentruber J, Renon H. Ind Engng Chem Res 1989;28:1049.
[27] Cheng HN, Khasat NP. J Appl Polym Sci 1988;25:825.
[28] Fischer D, Mülhaupt R. J Organomet Chem 1991;417:C7.
[29] Kaminsky W, Engehausen R, Zounis K, Spaleck W, Rohrmann J. Makromol Chem 1992;193:1643.
[30] Shin YS, Kim I, Lee JK, Won MS. J Polym Sci, Part A: Polym Chem 2000;38:1520.
[31] Packer KJ, Poplett JF, Taylor MJ, Vickers ME, Whittaker AK, Williams KP. J Makromol Chem Macromol Symp 1990;34:161.
[32] Wang LH, Poter RS, Stidham HD, Hsu SL. Macromolecules 1991;24:5535.
[33] Painter PC, Coleman MM, Koenig JL. The theory of vibrational spectroscopy and its application to polymeric materials. New York: Wiley, 1982. Chapter 3.
[34] Christopher CN, Robert JM, Bert JK, Kenneth PJ, Williams SM, Mason NC, Gerrard DL. Macromolecules 1995;28:2969.